Vibrothermography for NDT : dynamic control of thermal sources by acoustic fields

Hugo Boue, Adrien Arnaud, Anissa Méziane, Marie-Marthe Groz, Audrey Giremus, Emmanuelle Abisset-Chavanne

25-29 August 2024
inter.noise
NANTES FRANCE

Vibrothermography for NDT : dynamic control of thermal sources by acoustic fields

Hugo Boue[1],
Institute of mechanics and engineering (I2M)
Univ. Bordeaux, CNRS, Bordeaux INP, I2M, UMR 5295, F-33400, Talence, France
Arts et Metiers Institute of Technology, CNRS, Bordeaux INP, Hesam Universite, I2M, UMR 5295, F-33400 Talence, France

Adrien Arnaud[2]
Institute of mechanics and engineering (I2M)
Univ. Bordeaux, CNRS, Bordeaux INP, I2M, UMR 5295, F-33400, Talence, France
Arts et Metiers Institute of Technology, CNRS, Bordeaux INP, Hesam Universite, I2M, UMR 5295, F-33400 Talence, France

Anissa Meziane[3]
Institute of mechanics and engineering (I2M)
Univ. Bordeaux, CNRS, Bordeaux INP, I2M, UMR 5295, F-33400, Talence, France
Arts et Metiers Institute of Technology, CNRS, Bordeaux INP, Hesam Universite, I2M, UMR 5295, F-33400 Talence, France

Marie-Marthe Groz[4]
Institute of mechanics and engineering (I2M)
Univ. Bordeaux, CNRS, Bordeaux INP, I2M, UMR 5295, F-33400, Talence, France
Arts et Metiers Institute of Technology, CNRS, Bordeaux INP, Hesam Universite, I2M, UMR 5295, F-33400 Talence, France

Audrey Giremus[5]
Integration from material to system (IMS)
Univ. Bordeaux, CNRS, Bordeaux INP, IMS, UMR 5218, F-33400 Talence, France

Emmanuelle Abisset-Chavanne[6]
Institute of mechanics and engineering (I2M)
Univ. Bordeaux, CNRS, Bordeaux INP, I2M, UMR 5295, F-33400, Talence, France

[1]hugo.boue@u-bordeaux.fr
[2]adrien.arnaud.1@etu.u-bordeaux.fr
[3]anissa.meziane@u-bordeaux.fr
[4]marie-marthe.groz@u-bordeaux.fr
[5]audrey.giremus@u-bordeaux.fr
[6]emmanuelle.abisset-chavanne@ensam.eu

Arts et Metiers Institute of Technology, CNRS, Bordeaux INP, Hesam Universite, I2M, UMR 5295, F-33400 Talence, France

ABSTRACT

Among the plethora of Non-Destructive Testing techniques, the coupling of acoustic and thermography has emerged as a powerful method, more particularly denoted as sonothermography, utilizing the principle of energy conversion from acoustic waves to thermal heat sources to reveal structural abnormalities or create tunable volumic sources in materials. The calculation of the displacement field induced by acousto-vibrational excitations, using the analytical expression of energy conversion, has led to the generation and modeling of localized thermal sources in space over time within a material. By manipulating the input parameters of acoustic signals (frequency, phase, amplitude), we have demonstrated that it is possible to strategically position these sources in space and optimize the dissipation of thermal energy. The variation of parameters (creating a phase shift, a beat, a reversal law, etc.) makes it possible to control and move these internal heat sources to scan the material (in numerical approach and in the near future experimentally). The analysis of the resulting fields (acoustic-vibration and thermal), using inverse methods, opens up new possibilities for measuring the physical properties (mechanical, thermal) or characterizing defects in a material.

1. INTRODUCTION

Non-destructive Testing (NDT) methods play an essential role in examining and testing the integrity of materials and structures [1]. Numerous NDT methods are currently deployed in industry, but they reveal their limitations when the properties sought are manifested at different scales and are influenced by distinct physical dynamics within the material. Traditional techniques, relying on thermal [2] [3] [4] and ultrasonic approaches [5] [6] [7], have certain limitations. By combining these two physical approaches, it is possible to mitigate the drawbacks of each method. This hybrid method is called sonothermography [8] [9], thermoacoustic [10] or alternatively vibrothermography [11] [12]. In contrast to purely thermal NDT techniques, which involve inducing external thermal excitation at the surface of the material [13] [14], sonothermography allows volumetric heat sources to be generated inside the material. Ultrasonic NDT methods require the generation of high-frequency waves for defect charaterisation, but theses waves dissipate rapidly in the material, limiting defect detection to regions close to the surface. An additional advantage of sonothermography is its ability to excite and defects through the entire thickness of the material. In the presence of defects or depending on the material's inherent thermomechanical properties, such as viscoelasticity, a portion of the mechanical energy induced by wave propagation can be converted into thermal energy [8] [15] [9], leading to the generation of heat sources. Examining the resulting mechanical fields, including acoustic and thermal aspects, enables the estimation of material properties or defect characteristics using inverse methods [16], [17], [18]. In this publication, only the energy conversion linked to viscoelasticity will be considered.

Controlling and manipulating the resulting fields, both thermal and acoustic, is therefore the first step to the 3D characterization of a material. This process will facilitate real-time evaluation of a part to determine its global or local characteristics. This research focuses on the effect of different parameters on the efficiency of heat source generation based on acoustic data. In addition, a first approach is proposed by adding two out-of-phase excitation sources in order to move the position of the thermal sources.

2. ENERGY CONVERSION

One of the key concepts in sonothermography is the propagation of an acoustic wave in a material to generate and control heat sources. The wave generated by a piezoelectric transducer

is propagated through the material. In the presence of a defect, or of the material's viscoelasticity, part of the mechanical energy (induced by the wave's passage) is converted into thermal energy, resulting in the appearance of heat sources. The Figure 1 diagram illustrates the key points in the acoustic/thermal transition.

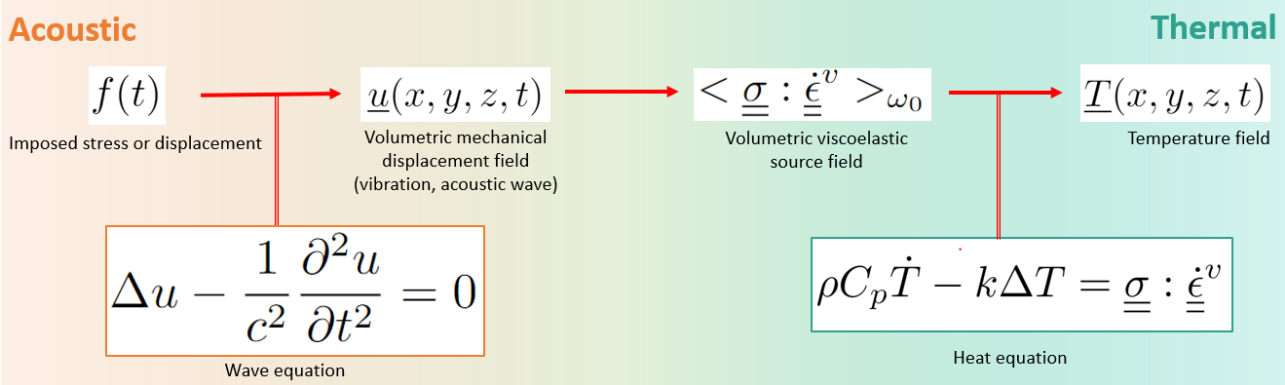

Figure 1: Diagram of the key points in the transition from acoustic excitation to the resulting thermal response.

2.1. Presentation of the hypothesis and the equations of energy conversion process

Firstly, let us outline the key steps and formulas to transition from deformation induced by an acoustic excitation source to a temperature field. The expression of the energy dissipation term (cf. Figure 1) stems from the energy balance [8]. Starting from the local writing of the first principle of thermodynamics and considering the virtual power theorem, the internal power is written in Equation 1 as follow:

$$Pi = -\int_{\Omega} \boldsymbol{\sigma} : \dot{\varepsilon} dV \tag{1}$$

Where Ω represents the sample volume to which the energy balance applies, σ corresponds to Cauchy stress tensor and $\dot{\varepsilon}$ conform to strain-rate tensor depending to displacement speed upon the passage of a disturbance (denoted v, where $v = \frac{\partial u(x,y,z,t)}{\partial t}$) as described in Equation 2 :

$$\dot{\varepsilon} = \frac{1}{2}\left(\nabla \boldsymbol{v}(\boldsymbol{x},\boldsymbol{y},\boldsymbol{z},\boldsymbol{t}) + (\nabla \boldsymbol{v}(\boldsymbol{x},\boldsymbol{y},\boldsymbol{z},\boldsymbol{t}))^T\right) \tag{2}$$

It is important to note that the strain rate $\dot{\varepsilon}$ is the sum of an elastic $\dot{\varepsilon}^e$ and viscoelastic $\dot{\varepsilon}^v$ component. The energy dissipation observed in the sonothermography mechanisme derives from the viscoelastic deformation term. Thus, by developing the energy balance, considering the specific internal energy per unit mass $e = f(s,\psi)$ as function of characteristic entropy (called s) and free energy (as illustrated by ψ), the heat equation is expressed in Equation 3:

$$\rho C_p \dot{T}(x,y,z,t) = \boldsymbol{\sigma} : \dot{\varepsilon}^v + k\Delta T(x,y,z,t) + r + T(x,y,z,t)\frac{\partial \sigma}{\partial T(x,y,z,t)} : \dot{\varepsilon}^e \tag{3}$$

Where ρ, C_p and k respectively represent the mass density in $[kg.m^{-3}]$, the specific heat at constant pressure $[J.kg^{-1}.K^{-1}]$, the conductivity $[W.m^{-1}.K^{-1}]$ and thermal volume source terms $\boldsymbol{\sigma} : \dot{\varepsilon}^v$ $[W.m^{-3}]$. Solving the heat equation with a source term (finite elements, finite volumes, analytical) results in the generation of a temperature field $T(x,y,z,t)[K]$ specific to the imposed mechanical excitation.

Now, it is necessary to establish the assumptions underlying the deformation source term. The assumptions are:

- Monochromatic acoustic excitation (denoted $f(t)$ in Figure 1). This excitation source corresponds to either a stress or an imposed displacement.
- Viscoelastic material behavior. Viscoelasticity in a material reflects an intermediate mechanical behavior between elastic and viscous behaviors. Moreover, viscoelastic deformation generates volumetric thermal sources. The movement generates friction between molecules and create volumetric thermal sources. This phenomenon is known as viscoelastic dissipation. The model used to model viscoelasticity is called hysteretic model as seen in references [9] [15].
- There is no internal generation of heat from external sources (hence $r = 0$). Thermomechanical coupling is negligibled, therefore $\frac{\partial \sigma}{\partial T(x,y,z,t)} = 0$. To simplify the problem, the material will be considered adiabatic and isotropic.
- Weak coupling between acoustic and thermal behavior. Acoustic variations occur on the order of microseconds, while thermal variations are on the order of tens of seconds. Therefore, this timescale difference between the two physical phenomena justifies the use, for thermal calculations, of an average value of the viscoelastic dissipation rate (as shown by the term $\langle \sigma : \dot{\varepsilon}^v \rangle_{f_0}$ in Figure 1).

According to the previous assumptions, since the excitation is monochromatic [9], it's possible to solve the wave equation in the frequency domain (by applying a Fourier transform illustrated by TF as $\tilde{X} = TF(X)$) to obtain a volumetric displacement $u(x,y,z,t)$ field. The viscoelastic strain rate amounts to a linear viscoelastic behavior, modeled by a complex stiffness tensor [15], is taken into account for the studied material [9] [16] as follows Equation 5 :

$$\tilde{\varepsilon} = \tilde{\varepsilon}^e + \tilde{\varepsilon}^v = S\tilde{\sigma} = (S' + iS'')\tilde{\sigma} \tag{4}$$

S is compliance matrix. Hence,

$$\tilde{\varepsilon}^v = S\tilde{\sigma} = iS''\tilde{\sigma} \tag{5}$$

In this work, the excitation source U_{CL} is positioned on one of the surfaces of the sample. For the boundary conditions, a displacement noted U_{CL} will be imposed on one of the sample surfaces along the z axis, of amplitude A, frequency f_0. This boundary condition is represented by the Equation 6:

$$U_{CL} = A\sin(2\pi f_0 t) \tag{6}$$

Therefore, for a monochromatic excitation Equation 6 passing into the frequency domain, it's possible to express the viscoelastic source term of a material as follows Equation 7:

$$\left\langle \sigma : \partial_t \varepsilon^v \right\rangle_{f_0} = \frac{-\omega_0 S''_{\alpha\beta}(\omega_0)}{2\pi} Re\left[\tilde{\sigma}_\alpha(\omega_0) \cdot \overline{\tilde{\sigma}_\beta(\omega_0)}\right] \tag{7}$$

With α and β as indices of Einstein notation, and the symbol $\overline{\sigma}$ represents the conjugate of the variable σ. This Equation 7 is a generic expression for viscoelastic heat sources. As such, it needs to be applied to a given sample. The behavioral law, material properties and geometry will determine the type of deformation, depending on the applied excitation.

2.2. Simulation of the temperature fields resulting from the propagation of ultrasonic waves through a PVC sample.

Figure 2 shows the material used for Finite Element simulation of viscoelastic heat sources. The model used in the finite element approach with COMSOL Multiphysics software was

Table 1: Geometric, mechanical and thermal properties of the studied PVC sample.

Material	Geometry [mm]	Mechanical properties	Thermal properties		
		Complex viscoelasticity modules [GPa]	Conductivity $[W.m^{-1}.K^{-1}]$	Heat capacity $[J.kg^{-1}.K^{-1}]$	Density $[g.m^{-3}]$
Polyvinyl chloride (PVC)	$L_x = 3$	$C_{11} = C_{22} = 7.9(1+0.03i)$	$k = 0.1$	$C_p = 1000$	$\rho = 1.17$
	$L_y = 20$	$C_{66} = 1.6(1+0.03i)$			
	$L_z = 120$	$C_{12} = C_{11} - 2C_{66}$			

developed in [9]. Firstly, by solving the wave equation as a partial differential equation in the Fourier frequency domain, the displacement field induced by monochromatic harmonic loading can be determined. Then, using the Heat Transfer module and the viscoelasticity formula mentioned in Equation 7, the temperature field is calculated.

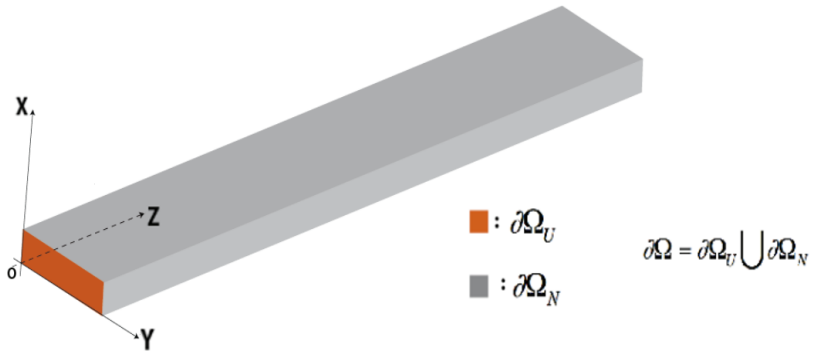

Figure 2: Schematic diagram of the study area and boundary conditions (in orange).

The sample studied is PVC, the material and physical properties of which are listed in the Table 1.

Modal analysis was performed at a resonant frequency, facilitating resonance phenomena within the sample and driving high-amplitude magnitudes. The chosen resonance frequency maximizes the displacement of the structure. Consequently, the rate of deformation will be maximum, delivering a significant rise in temperature at the surface of the material. In this study, only stationary compression/traction waves will be considered. A displacement imposed on the boundary $\partial\Omega_U$ in Figure 2 is considered with a frequency of $f_0 = \dfrac{\omega_0}{2\pi} = 27$ kHz and displacement amplitude of $A = 400$nm.

By estimating the displacement field resulting from the excitation $f(t)$ in $\partial\Omega_U$, it is possible to calculate strain rates $\dot{\varepsilon}^v$ throughout the material. Then, by solving the heat equation Equation 3 with a dissipative source term $\langle \sigma : \dot{\varepsilon}^v \rangle_{f_0}$, the Figure 3 depicted the temperature rise obtained at the surface of the material.

Taking the central line on the upper surface of the sample (red segment in the Figure 3), the Figure 4 illustrate the links between displacement, deformation and viscoelastic sources. In this scenario, at a vibrating node, the deformation rate reaches its maximum, resulting in the presence of a thermal source.

3. RESULTS

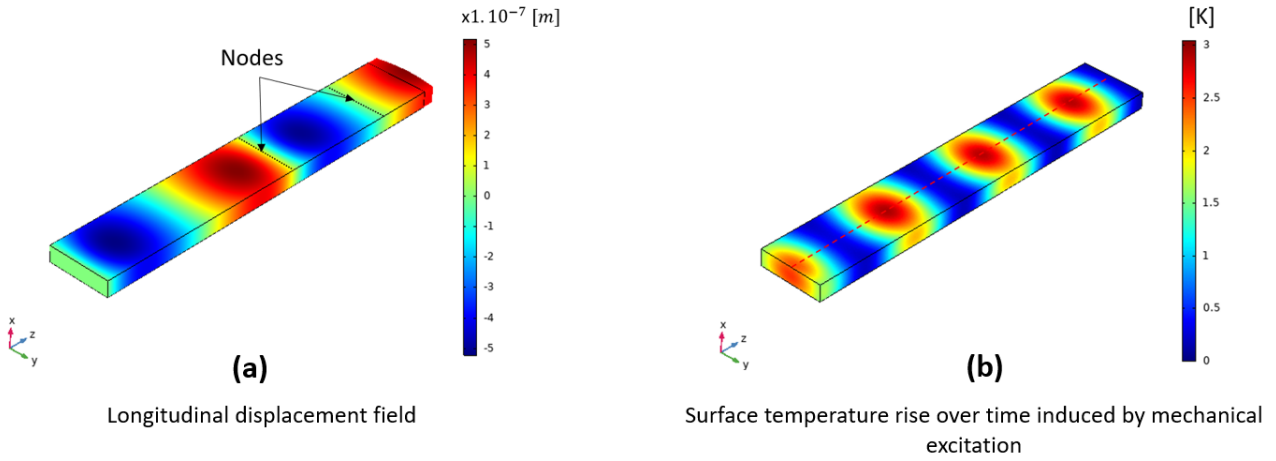

Figure 3: **(a)** the displacement field calculated for a stationary compression wave along z and **(b)** the temperature field at the surface of the material generated by this mechanical excitation.

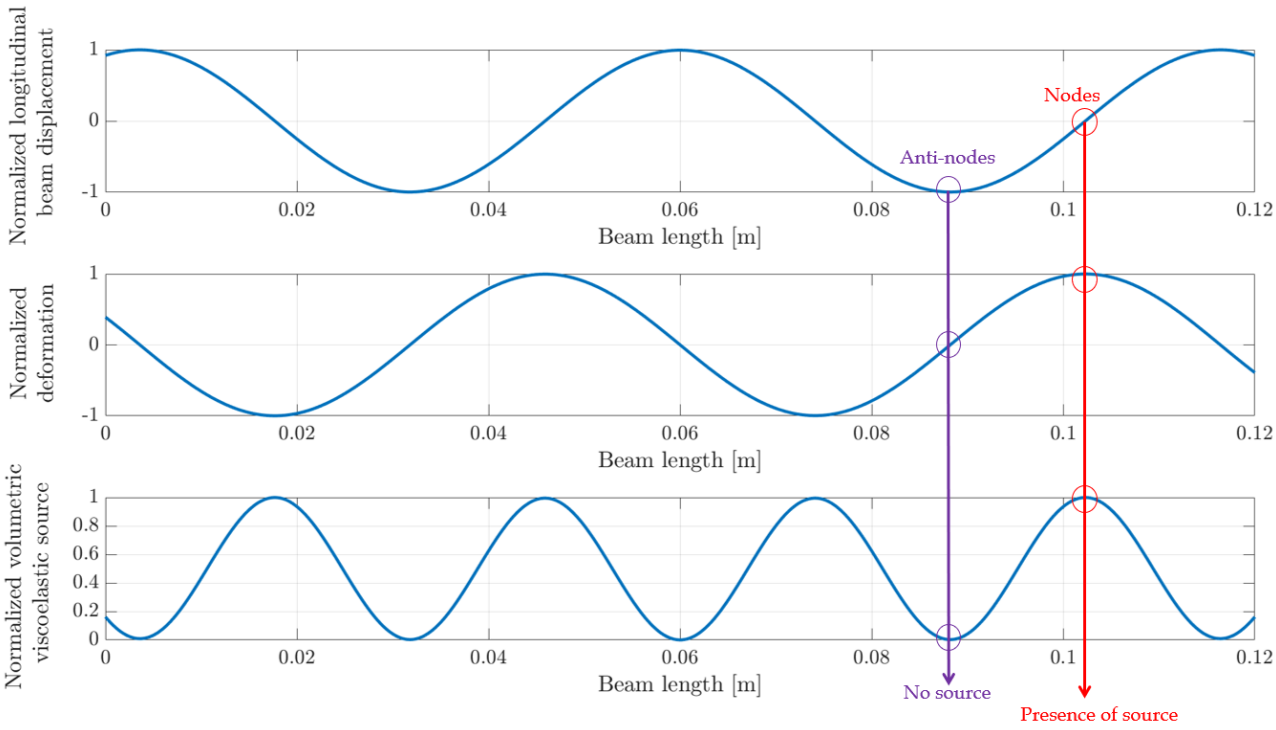

Figure 4: Displacement, deformation and viscoelastic volume source field along the neutral axis as a function of beam length.

3.1. Experimental validation of heat source position

Experimental measurements carried out with the set-up (illustrated by Figure 5) confirmed that the source terms are positioned on vibration nodes. The measuring bench consists of a PVC sample positioned between two measuring devices. Above the PVC, a FLIR infrared camera positioned at a distance of 20 cm measures the temperature elevation on the surface of the material. A 3D laser vibrometer with 3 laser (POLYTECH PSV-500-3D) heads at a wavelength of 534 nm measures displacement velocity fields in 3 spatial directions on the surface of the material. At the extremity of the PVC sample, a piezoelectric acoustic actuator excites the structure. The latter receives the excitation signal via a GBF (low-frequency generator), which is then amplified

by an amplifier (CEDRAT TECHNOLOGIES LA75). To accomplish this, as illustrated in Figure 5, a

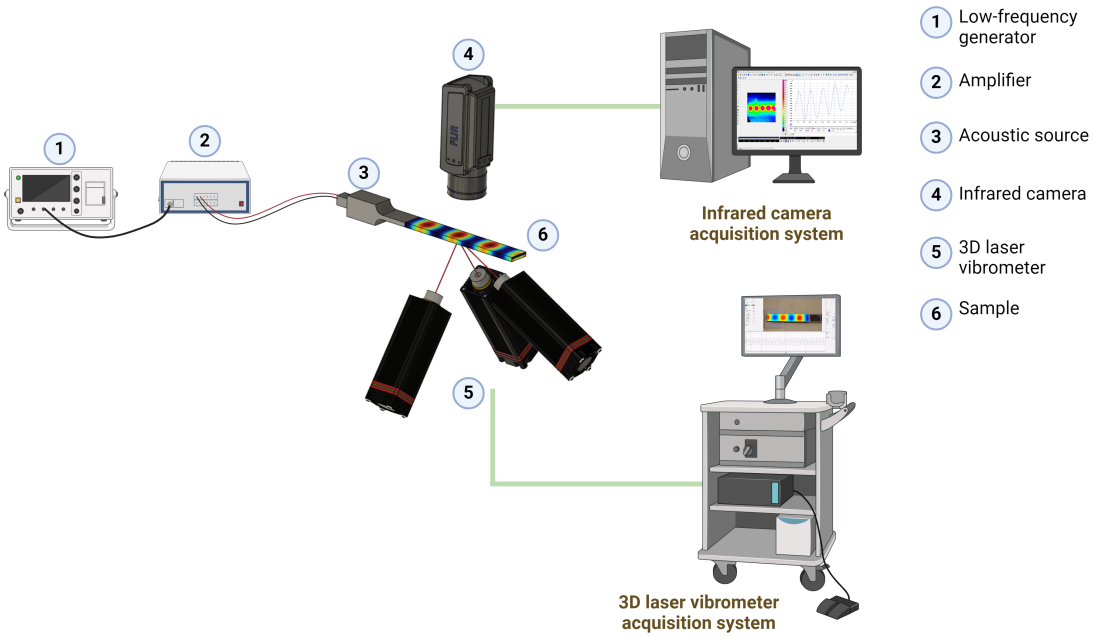

Figure 5: Experimental set-up.

PVC sample, with its geometric and physical attributes detailed in Table 1, is utilized. In order to recover the mode simulated in section 2, due to the coupling conditions, the resonance frequency is experimentally recovered and corresponds to $f_0 = 32kHz$. All measurements are made at the surface of the material, as indicated by the red line in the Figure 3, to limit 3D effects.

Using a 3D laser vibrometer, laser interferometry measurements were applied to characterize in-plane displacement and displacement velocity at any point of the surface of the sample. Assuming that the cross-section of the (x, y) plane in Figure 2 moves homogeneously, the final displacement is represented in blue on the Figure 6. Both antinodes and nodes are clearly visible. An infrared camera placed above the sample (as depicted in Figure 5) enable to observe the temperature rises linked to the thermal sources generated by acoustic waves. The temperature rise is shown in figure 6 by red curve. The nodes (i.e. the intersection between the blue and black lines represented by the black circles in Figure 6) correspond to a local maximum temperature rise (red curve). Displacement and velocity amplitudes are of the same order of magnitude as those obtained with the finite element model. However, the difference can be explained by the experimental boundary conditions. The interaction between the acoustic actuator and the sample is a hypothesis to explain this difference. Within a NDT framework, obtaining a localized estimation of the parameter of interest involves relocating the nodes and, consequently, the heat sources to the desired location. However, experimental control of the positioning and intensity of heat sources proves challenging. For this reason, a simplified 1D approach is suggested, employing an analytical model assuming a beam structure. The objective is to explore the impact of various acoustic signal input parameters such as frequency, phase, amplitude, and others.

3.2. Displacement of sources by varying the phase

In order to move the sources, several strategies are available: the frequency, the phase, the signal amplitude, number of acoustic exciter sources and the type of excitation. This takes advantage of the resonance of the structure and assumes monochromatic excitation, the study will focus exclusively on the phase variation between two signals. As indicated in Figure 7, a second source is positioned at $z = L$. This second source emits a sinusoidal wave whose phase

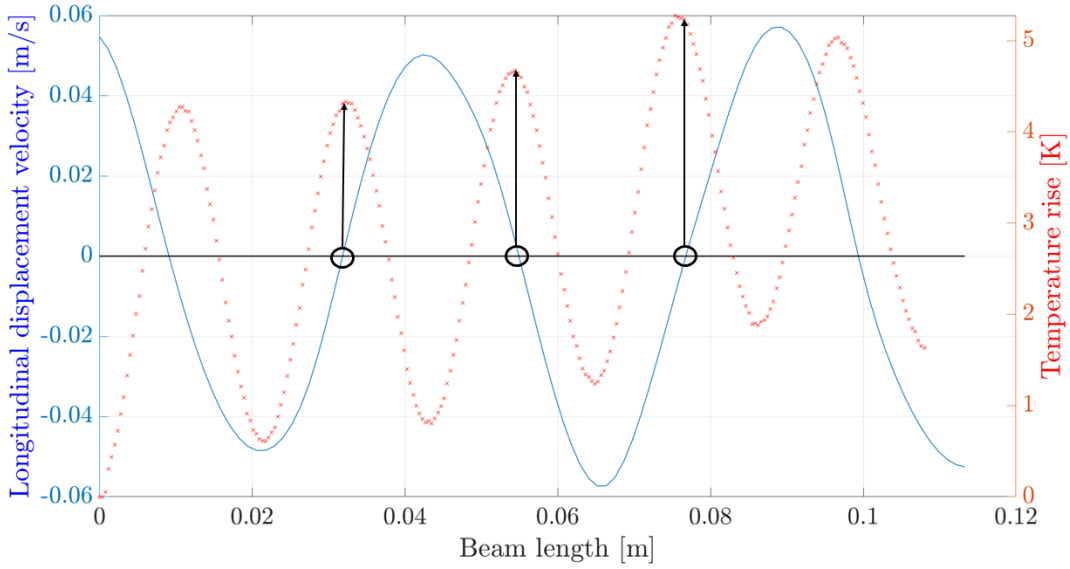

Figure 6: Superposition of temperature fields and displacement velocities along a neutral line on the material surface.

shift ϕ can vary between $[0\,;\pi]$ and over time.

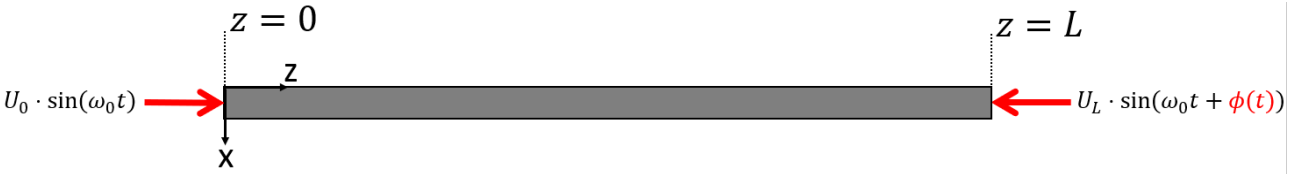

Figure 7: Schematic representation of a beam of length L subjected to 2 phased excitations.

The resulting displacement field is expressed by Equation 8:

$$U_z(z,t) = e^{i\omega_0.t}.(U_L\frac{\sin(k'z)}{\sin(k'L)}e^{i\phi} + U_0.\frac{\sin(k'(L-z))}{\sin(k'L)}) \tag{8}$$

Where $L = L_z$ cm represents the length of the material, U_0 and U_L represent the amplitudes in [nm] of the different sources, and U_z represents the total displacement of the 1D beam along z.

This material being isotropic, knowing the associated behavior law, it is possible to write that the thermal source field averaged over a one-dimensional period for two excitations is expressed in Equation 9 as:

$$\left\langle \sigma : \partial_t \varepsilon^v \right\rangle_{\omega_0} = \frac{\omega_0}{2\pi^2}.C_{33}^{"}.|\varepsilon_{33}(z)|^2 = \frac{\omega_0}{2\pi^2}.C_{33}^{"}.|\frac{k'}{\sin(k'L)}.(U_L\cos(k'z)e^{i\phi} - U_0.\cos(k'(L-z)))|^2 \tag{9}$$

Where $C_{33}^{"}$ represents the complex part of the elasticity tensor.

The phase shift occurs over time in Figure 8. Note that the amplitude of the source also varies according to the ϕ phase of the second source. It is observed that a phase shift of π allows sweeping half a wavelength. At this frequency, this sweeping allows heating any point of the beam. The displacement of the center of the sources depends on half the wavelength. In this example, a displacement of the nodes and consequently of the thermal sources in the material of around 0.018 m (corresponding to a quarter wavelength) is observed (represented by the black arrows in the Figure 8).

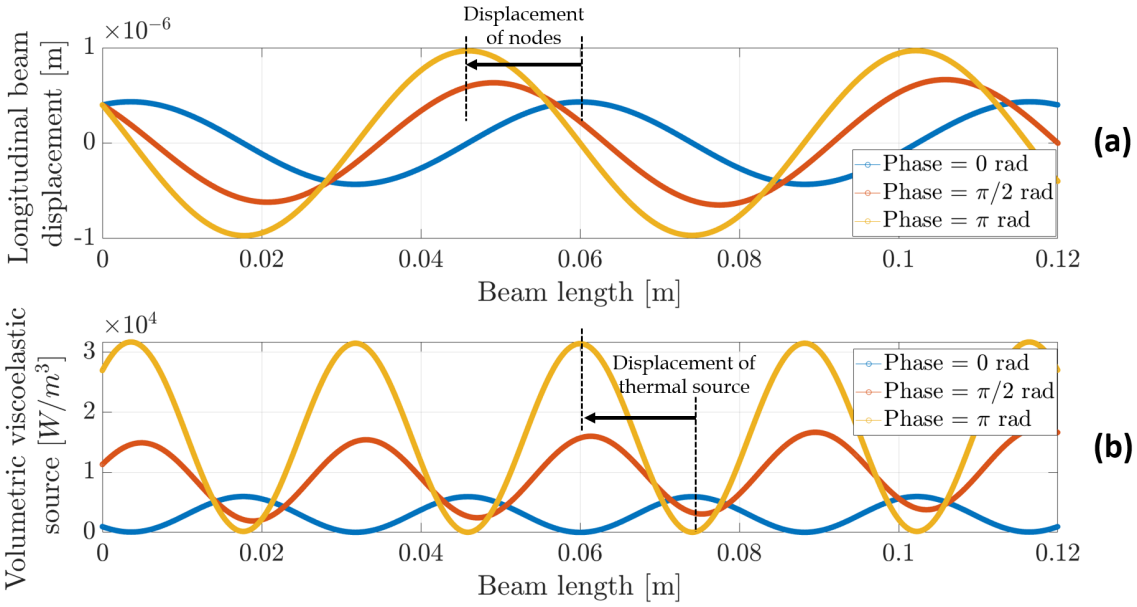

Figure 8: **(a)** Displacement of acoustic fields (nodes) and **(b)** viscoelastic source in the material at a frequency of $f_0 = 27KHz$.

4. CONCLUSION

In conclusion, this work has demonstrated, either analytically or using finite element models, the strong correlation between the position of volume sources and vibration nodes within the framework of a beam under a standing wave hypothesis. Experimental validation has enabled the deployment of an experimental setup for measuring high-precision acoustic and thermal fields. In addition, a numerical study was carried out to control and move thermal sources using purely acoustic data. By varying not only the phase, but also the frequency or amplitude of the acoustic signals, it is possible to heat sources in the volume and move them over a distance of half a wavelength. Work is in progress to demonstrate the control and displacement of heat sources using two phase-shifted excitations on the PVC sample.

ACKNOWLEDGEMENTS

This research was supported by "Projet Région Nouvelle-Aquitaine" and l'Agence de l'innovation de défense (AID) funding. We would also like to thank the "Réseau de Recherche Impulsion BEST Usine du futur" for funding and enabling us to carry out this work.

REFERENCES

1. Sophian A. Non-destructive testing (NDT) in industry 4.0: A brief review.
2. Malo Lecorgne, Emmanuelle Abisset-Chavanne, Marie-Marthe Groz, Alain Sommier, and Christophe Pradère. A study on real-time quantitative thermal analysis of composite tapes. *NDT & E International*, page 103096, 2024.
3. WJ Parker, RJ Jenkins, CP Butler, and GL Abbott. Flash method of determining thermal diffusivity, heat capacity, and thermal conductivity. *Journal of applied physics*, 32(9):1679–1684, 1961.
4. DL Balageas. Nouvelle méthode d'interprétation des thermogrammes pour la détermination de la diffusivité thermique par la méthode impulsionnelle (méthode «flash»). *Revue de Physique Appliquée*, 17(4):227–237, 1982.
5. M. Friedrich-Rust, Katrin Wunder, S. Kriener, Fariba Sotoudeh, S. Richter, J. Bojunga,

E. Herrmann, T. Poynard, C. Dietrich, J. Vermehren, S. Zeuzem, and C. Sarrazin. Liver fibrosis in viral hepatitis: noninvasive assessment with acoustic radiation force impulse imaging versus transient elastography. *Radiology*, 252 2:595–604, 2009.

6. A. Sarvazyan, M. Urban, and J. Greenleaf. Acoustic waves in medical imaging and diagnostics. *Ultrasound in medicine biology*, 39 7:1133–46, 2013.
7. Morcos L Wanis, Jennifer A Wong, Samuel Rodriguez, Jasmine M Wong, Brice Jabo, Arjun Ashok, Sharon SJ Lum, Naveenraj L Solomon, Mark E Reeves, Carlos A Garberoglio, et al. Rate of re-excision after breast-conserving surgery for invasive lobular carcinoma. *The American Surgeon*, 79(10):1119–1122, 2013.
8. Thermal characterization of viscoelastic materials using sonothermography. 1581.
9. M Castaings, C Bacon, B Hosten, and MV Predoi. Finite element predictions for the dynamic response of thermo-viscoelastic material structures. *The Journal of the Acoustical Society of America*, 115(3):1125–1133, 2004.
10. Mehdi Naderi, Ali Kahirdeh, and Michael M Khonsari. Dissipated thermal energy and damage evolution of glass/epoxy using infrared thermography and acoustic emission. *Composites Part B: Engineering*, 43(3):1613–1620, 2012.
11. Jyani S Vaddi, Stephen D Holland, and Michael R Kessler. Absorptive viscoelastic coatings for full field vibration coverage measurement in vibrothermography. *NDT & E International*, 82:56–61, 2016.
12. Jeremy Renshaw, Stephen D Holland, and Daniel J Barnard. Viscous material-filled synthetic defects for vibrothermography. *Ndt & E International*, 42(8):753–756, 2009.
13. L Gaverina, JC Batsale, A Sommier, and Christophe Pradere. Pulsed flying spot with the logarithmic parabolas method for the estimation of in-plane thermal diffusivity fields on heterogeneous and anisotropic materials. *Journal of Applied Physics*, 121(11), 2017.
14. Agustín Salazar, Arantza Mendioroz, and Alberto Oleaga. Flying spot thermography: Quantitative assessment of thermal diffusivity and crack width. 127(13). Publisher: American Institute of Physics Inc.
15. Miguel A Torres-Arredondo and C-P Fritzen. A viscoelastic plate theory for the fast modelling of lamb wave solutions in ndt/shm applications. *Ultragarsas/Ultrasound*, 66(2):7–13, 2011.
16. Clément Despres, Christine Biateau, Michel Castaings, Nicolas Quaegebeur, Patrice Masson, and Eric Ducasse. Characterization of viscoelastic moduli and thickness of isotropic, viscoelastic plates using multi-modal lamb waves. *NDT & E International*, page 103095, 2024.
17. Hugo Boue, Marie-Marthe Groz, E Abisset-Chavanne, A Giremus, and A Meziane. Reconstruction of buried thermal sources from surface temperature fields by bayesian inference. *Computational Thermal Sciences: An International Journal*, 16(1), 2024.
18. S Löhle, U Fuchs, P Digel, T Hermann, and J-L Battaglia. Analysing inverse heat conduction problems by the analysis of the system impulse response. *Inverse Problems in Science and Engineering*, 22(2):297–308, 2014.